BIOCHEMISTRY
including biophysical chemistry & molecular biology

Article

pubs.acs.org/biochemistry

Infrared Detection of a Proton Released from Tyrosine Y_D to the Bulk upon Its Photo-oxidation in Photosystem II

Shin Nakamura and Takumi Noguchi*

Division of Material Science, Graduate School of Science, Nagoya University, Furo-cho, Chikusa-ku, Nagoya, 464-8602, Japan

Supporting Information

ABSTRACT: Photosystem II (PSII) has two symmetrically located, redox-active tyrosine residues, Y_Z and Y_D. Whereas Y_Z mediates the electron transfer from the water-oxidizing center to P680 in the main electron transfer pathway, Y_D functions as a peripheral electron donor to P680. To understand the mechanism of this functional difference between Y_Z and Y_D, it is essential to know where the proton is transferred upon its oxidation in the proton-coupled electron transfer process. In this study, we used Fourier transform infrared (FTIR) spectroscopy to examine whether the proton from Y_D is released from the protein into the bulk. The proton detection method previously used for water oxidation in PSII [Suzuki et al. (2009) *J. Am. Chem. Soc. 131*, 7849−7857] was applied to Y_D; a proton released into the bulk upon Y_D oxidation was trapped by a high-concentration Mes buffer, and the protonation reaction of Mes was monitored by FTIR difference spectroscopy. It was shown that 0.84 ± 0.10 protons are released into the bulk by oxidation of Y_D in one PSII center. This result indicates that the proton of Y_D is not transferred to the neighboring D2-His198 but is released from the protein; this is in sharp contrast to the Y_Z reaction, in which a proton is transferred to D1-His190 through a strong hydrogen bond. This functional difference is caused by differences in the hydrogen-bonded structures of Y_D and Y_Z, which are determined by the hydrogen bond partners at the N_π sites of these His residues, i.e., D2-Arg294 and D1-Asn298, which function as a hydrogen bond donor and acceptor, respectively. This FTIR spectroscopy result supports the recent theoretical prediction [Saito et al. (2013) *Proc. Natl. Acad. Sci. U.S.A. 110*, 7690−7695] based on the X-ray crystallographic structure of PSII and explains the different rates of the redox reactions of Y_D and Y_Z.

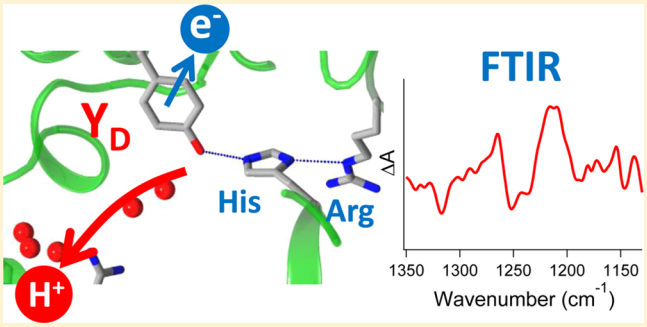

Photosystem II (PSII) is a multisubunit pigment protein complex that functions in light-driven water oxidation. Upon absorption of light, charge separation between the chlorophyll dimer P680 and pheophytin electron acceptor (Pheo) occurs, leading to the formation of $P680^+Pheo^-$.[1,2] The redox-active tyrosine Y_Z (D1-Tyr161) donates an electron to $P680^+$ at 30 ns to 50 μs,[3,4] which then abstracts an electron from the Mn_4CaO_5 cluster, the core part of the water-oxidizing center (WOC), at the rates of 30 μs to 2 ms, depending on different intermediates, called S_i states (i = 1−4), of the WOC.[5−8] There is another redox-active tyrosine, Y_D (D2-Tyr160), which is located symmetrically to Y_Z, on the electron-donor side of PSII.[3,9] In contrast to Y_Z, however, Y_D functions as a peripheral electron donor to $P680^+$ and has only a weak interaction with the Mn_4CaO_5 cluster.[10,11] The rate of electron transfer from Y_D to $P680^+$ is in the millisecond regime,[12,13] which is much slower than that from Y_Z. In addition, the oxidized Y_D is significantly stable at room temperature and rereduced by the S_0 state of WOC in hours.[10,11] Although the exact physiological role of Y_D remains unclear, it has been suggested that Y_D serves functions related to maintaining the WOC in stable higher valence states by oxidation of the overreduced forms, affecting the energetics of $P680^+$, accelerating the photoactivation process of WOC, and protecting against photoinhibition.[14−16] The remaining question concerns the mechanistic cause of the expression of this significant functional difference between Y_Z and Y_D despite their symmetrical locations in PSII.[3,9,12,17]

It is well-known that both Y_Z and Y_D perform proton-coupled electron transfer reactions.[3,9,12,16−27] When they are oxidized, the proton of the phenolic group is released and neutral Try radicals, $Y_Z^\bullet$ and $Y_D^\bullet$, are formed. The X-ray crystallographic structures of PSII complexes showed that the N_τ nitrogen of the imidazole group of D1-His190 and D2-His189 is located in close vicinity to the phenolic oxygen of Y_Z and Y_D, respectively (Figure 1),[28−31] and it most probably forms a hydrogen bond.[16−27] Thus, it has been thought that these His side chains function as proton acceptors of Y_Z and Y_D. Indeed, there are several lines of experimental and theoretical evidence that a proton moves back and forth between Y_Z and D1-His190 through a strong hydrogen bond upon oxidation and rereduction.[9,24,25,27,32−35] This proton-rocking mechanism explains the rapid proton-coupled electron transfer reactions of Y_Z. Recently, we directly detected the proton transferred from Y_Z to D1-His190 as its N_τ-H stretching

Received: May 25, 2015
Revised: August 4, 2015
Published: August 4, 2015

DOI: 10.1021/acs.biochem.5b00568
Biochemistry 2015, 54, 5045−5053

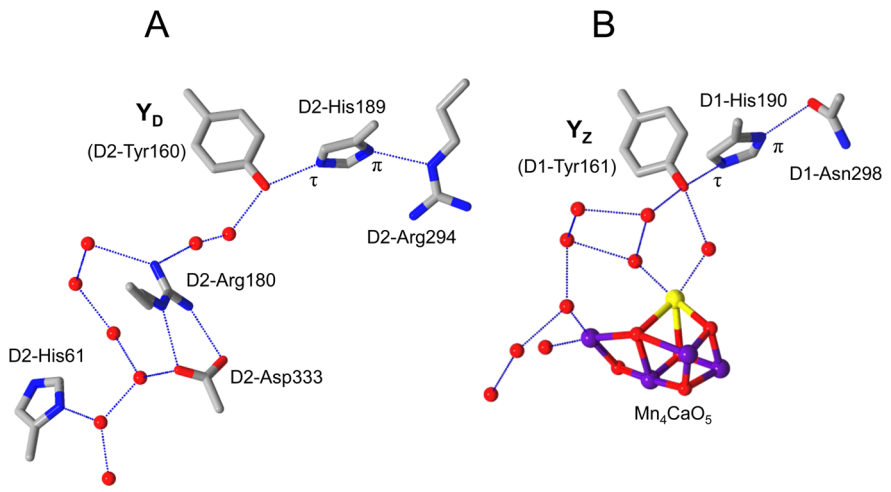

Figure 1. Molecular interactions and hydrogen bond networks of Y_D (A) and Y_Z (B) in the X-ray crystallographic structure of PSII complexes (PDB code: 3ARC[30]).

vibration at ~2800 cm^{-1} using light-induced Fourier transform infrared (FTIR) difference spectroscopy.[27] A corresponding NH band was absent in the FTIR difference spectra of Y_D,[27] suggesting the difference in the hydrogen-bonded structure and proton transfer mechanism between Y_Z and Y_D. It has also been suggested that some other nearby residues function as proton acceptors of Y_D.[36,37] Saito et al.[17] performed theoretical calculations of Y_D reactions using the high-resolution (1.9 Å) X-ray structure of PSII. The result showed that when Y_D was oxidized, its proton is transferred away from Y_D to the luminal side through a water chain near Y_D, and they suggested that this long-distance proton transfer is the cause of the much slower rate of the Y_D reaction compared with that of the Y_Z reaction.

To understand the mechanism of the functional difference between Y_Z and Y_D in PSII, it is crucial to experimentally monitor the fate of the proton released from Y_D upon its photooxidation and to determine whether the proton is released from the protein or trapped in a certain residue in the protein. In the present study, we estimated the number of protons released into the bulk upon Y_D oxidation using light-induced FTIR difference spectroscopy. FTIR spectroscopy has been extensively used to examine the reactions of redox cofactors in PSII,[38−47] and virtually all the changes coupled with the cofactor reactions, which involve changes in protein moieties, water molecules, electron donor and acceptors, and buffer molecules, have been detected. We employed the method that was previously used for the detection of protons from WOC during water oxidation:[48] protons trapped by the Mes buffer were monitored by isotope-edited Mes signals in light-induced FTIR difference spectra. The results showed that the proton from Y_D is released from the protein upon oxidation, supporting the theoretical prediction by Saito et al.[17] The structural factors contributing to the difference in the proton transfer reactions of Y_Z and Y_D and their relevance to the functions of these Tyr residues are discussed.

MATERIALS AND METHODS

PSII core complexes of *Thermosynechococcus elongatus*, in which the C-terminus of the CP47 subunit was histidine tagged,[49] were isolated following the method described previously.[27] Mn depletion was performed by 10 mM NH_2OH treatment for 30 min at room temperature. The Mn-depleted core complexes were then washed more than four times with a buffer containing 1 mM Mes-NaOH (pH 6.5), 5 mM NaCl, and 0.06% DM by ultrafiltration (Vivaspin 500; 100 kDa MWCO; Sartorius Stedim) to be finally concentrated to 3 mg chlorophyll/mL.

For $Y_D^{\bullet}/Y_D$ FTIR measurements, an aliquot (5 μL) of the Mn-depleted PS II sample (3 mg chlorophyll/mL) in the 1 mM Mes buffer mentioned above was mixed with 1 μL of 20 mM potassium ferricyanide, 1 μL of 40 mM potassium ferrocyanide, and 2 μL of 200 mM Mes or Mes-d_{12} (pH 6.5).[48] The Mes-d_{12} buffer was prepared by dissolving all-deuterated Mes (Mes-d_{13}: Cambridge Isotope Laboratories, Inc., 98% D) in H_2O, where the sulfonic acid group is ionized. To make a hydrated film, the sample was first dried on a BaF_2 plate (25 × 25 mm^2) under a N_2 gas flow and then sealed with another BaF_2 plate and a silicone spacer (0.5 mm in thickness). In the sealed cell, 2 μL of 40% (v/v) glycerol/H_2O was enclosed without touching the sample to produce 95% relative humidity.[50] The sample cell was cooled to 10 °C by circulating the cold water in a copper holder.

Light-induced FTIR spectra were recorded on a Bruker IFS-66/S spectrophotometer equipped with an MCT detector (D313-L). Flash illumination was performed using a Q-switched Nd:YAG laser (Quanta-Ray INDI-40-10; 532 nm; ~7 ns full-width at half-maximum; ~7 mJ $pulse^{-1}$ cm^{-2}). For $Y_D^{\bullet}/Y_D$ difference spectra, single-beam spectra with 100 scans (50 s accumulation) were recorded twice before illumination, once after one flash, and once after additional five flashes (1 Hz). This measurement was repeated 100 times with a dark interval of 450 s, and the spectra were averaged. Note that $Y_D^{\bullet}$ was rereduced by ferrocyanide ($\tau \sim 200$ s) during this dark interval. The $Y_D^{\bullet}/Y_D$ difference spectrum was obtained by taking the difference between the spectra after the first flash and the next five flashes, whereas the difference between the two spectra before illumination represents a noise level and a background change. The spectrum upon the first flash involves the contamination of the Fe^{2+}/Fe^{3+} signal of the nonheme iron on the electron acceptor side[51,52] because the nonheme iron was partially preoxidized in the ferricyanide/ferrocyanide redox couple and accepted an electron at the first flash. However, the signals of the nonheme iron were not involved after the second flash because it was fully reduced by the first flash. By contrast, the quantum efficiency of Y_D oxidation is relatively low; hence, full accumulation of the oxidized $Y_D^{\bullet}$ requires several flashes.

DOI: 10.1021/acs.biochem.5b00568
Biochemistry 2015, 54, 5045−5053

Thus, the difference spectrum by the next five flashes provided a pure $Y_D^{\bullet}/Y_D$ spectrum without contamination of the nonheme iron. There was no contribution of the signals from Y_Z and the Q_A and Q_B electron acceptors because of the fast relaxation of $Y_Z^{\bullet}$ at 10 °C and the quick electron transfer from the quinone to ferricyanide, which was confirmed by the absence of signals typical of $Y_Z^{\bullet}$ (CO stretch at 1515 cm^{-1}) and $Q_{A(B)}^{-}$ (CO/CC stretch at ~1480 cm^{-1}). Because reduction of the nonheme iron is known to accompany the uptake of a proton,[53] we abandoned the difference spectrum by the first flash and that by the next five flashes was adopted as a $Y_D^{\bullet}/Y_D$ difference spectrum to estimate the number of protons from Y_D.

For measurements of the FTIR difference spectra upon water oxidation at WOC, PSII complexes were washed with a buffer containing 1 mM Mes-NaOH (pH 6.5), 5 mM NaCl, 5 mM $CaCl_2$, and 0.06% DM and were concentrated to 3 mg chlorophyll/mL by ultrafiltration. An aliquot (5 μL) of a PSII suspension was mixed with 1 μL of 100 mM potassium ferricyanide and 2 μL of 200 mM Mes or Mes-d_{12} (pH 6.5).[48] A hydrated film was prepared using the same procedure used for the Y_D measurements. The sample temperature was maintained at 10 °C. Single-beam spectra with 40 scans (20 s accumulation) were recorded twice before flashes and once after 12 flashes (1 Hz). The measurement was repeated six times with a dark interval of 90 min. The spectra were averaged for the calculation of a light-minus-dark difference spectrum.

$Y_Z^{\bullet}/Y_Z$ FTIR spectra were measured following the method described previously[27] with slight modification. An aliquot (6 μL) of Mn-depleted PSII core complexes (6 mg chlorophyll/mL) in a buffer containing 1 mM Mes-NaOH (pH 6.5), 40 mM sucrose, 10 mM NaCl, 5 mM $MgCl_2$, and 0.06% DM was mixed with 1 μL of 100 mM potassium ferricyanide and 1 μL of 200 mM Mes or Mes-d_{12} (pH 6.5). After the sample was dried on a BaF_2 plate (13 mm in diameter) under a N_2 gas flow, it was mixed with 1 μL of 200 mM Mes or Mes-d_{12} (pH6.5) and then sandwiched with another BaF_2 plate. The sample temperature was adjusted to 250 K in a cryostat (Oxford DN1704). Single-beam spectra with 50 scans (25 s accumulation) were recorded twice before and once after applying a single flash. This measurement was repeated 400 times with a dark interval of 225 s, and the average spectra were used to calculate a $Y_Z^{\bullet}/Y_Z$ spectrum.

Spectral fitting to estimate the number of protons trapped by Mes was performed using Igor Pro (WaveMetrics Inc.). The regions of 1330−1150 and 2800−2400 cm^{-1} were separately fitted, and the estimated values were averaged to obtain a final value.

RESULTS

In this study, we applied the proton detection method using FTIR spectroscopy, which was developed by Suzuki et al.[48] to monitor the proton release during water oxidation at WOC, to the proton release from Y_D upon its photo-oxidation. In this method, protons released from PSII core complexes into the bulk were trapped by a high-concentration Mes buffer, and the protonation reaction of a Mes molecule (Figure 2) was monitored by FTIR difference spectroscopy. The FTIR signals of only Mes molecules were obtained by taking a double difference between Mes and deuterated Mes (Mes-d_{12}) to cancel the protein bands. At the same time, electron transfer was monitored using the CN stretching band of ferricyanide, which functions as an exogenous electron acceptor of PSII.

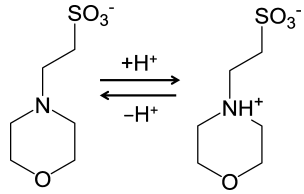

Figure 2. Protonation and deprotonation reactions of a Mes molecule.

Thus, the number of protons released from PSII during one turnover reaction of electron transfer can be estimated.[48]

$Y_D^{\bullet}/Y_D$ difference spectra were measured using a hydrated film of PSII complexes.[54,27] The CN band of ferricyanide at 2115 cm^{-1} was slightly wider in the hydrated film than in the solution sample previously used.[48] Thus, we first performed proton detection from WOC using the film sample to determine the standard intensity of the Mes signal relative to the intensity of the ferricyanide band for the same amounts of Mes and ferricyanide. Because water oxidation at WOC generates four protons and four electrons by one S-state cycle, the numbers of protons and electrons from WOC should be identical when a relatively large number of flashes are applied to PSII.

Figure 3 shows FTIR difference spectra of WOC upon illumination of 12 flashes on the PSII samples in Mes (a, black line) and Mes-d_{12} (a, red line) buffers (Figure 3A, 1800−1130 cm^{-1}; Figure 3B, 3000−2150 cm^{-1}). The spectra in trace a are normalized at the ferricyanide band at 2115 cm^{-1} (Figure 3C). (Note that the ferricyanide peak was used for normalization rather than the stronger ferrocyanide peak at 2038 cm^{-1} because the latter signal often changes the shape depending on the condition.[48]) The spectra represent the structural difference between the dark stable S_1 state and randomized S states as well as protonation of the Mes buffer by protons produced by water oxidation. The frequency region lower than 1130 cm^{-1}, which was used in the previous proton detection study,[48] was not shown in Figure 3 because the spectra in this region were found to be slightly saturated because of the relatively low sensitivity of the MCT detector and the large buffer absorption. In the present study, in addition to the mid-infrared region (Figure 3A), the high-frequency region (3000−2150 cm^{-1}; Figure 3B) was newly used for detection of proton release. This region involves the vibrations of the CH stretches (~2840 cm^{-1}), the NH stretch (2800−2400 cm^{-1}) probably coupled with the overtones and combinations of lower-frequency vibrations, and the CD stretches (2270−2220 cm^{-1}) of Mes and/or Mes-d_{12}. The merit of using this high-frequency region is that major protein bands of WOC and Y_D are absent;[27,55] hence, the bands of Mes buffer mostly appear in this region. The Mes-only signals without protein contributions were obtained in a Mes-minus-Mes-d_{12} double difference spectrum (Figure 3A,B; trace b). It was shown that the bands of Mes affected by its protonation are located in frequencies lower than 1350 cm^{-1} and higher than 2200 cm^{-1}.

Figure 4 shows $Y_D^{\bullet}/Y_D$ FTIR difference spectra of PSII samples in Mes (a, black line) and Mes-d_{12} (a, red line) buffers (Figure 4A, 1800−1130 cm^{-1}; Figure 4B, 3000−2150 cm^{-1}). These spectra are virtually identical to the previously reported $Y_D^{\bullet}/Y_D$ difference spectra.[21,27,37,54,56−60] The positive peak at 1504 cm^{-1} and the negative peak at 1255 cm^{-1} originate from the CO stretch of $Y_D^{\bullet}$ and the coupled mode of the CO stretch/COH bend of Y_D, respectively.[37,57,61] The Mes-minus-Mes-d_{12} double difference spectrum of Y_D (Figures 4A,B; trace

DOI: 10.1021/acs.biochem.5b00568
Biochemistry 2015, 54, 5045−5053

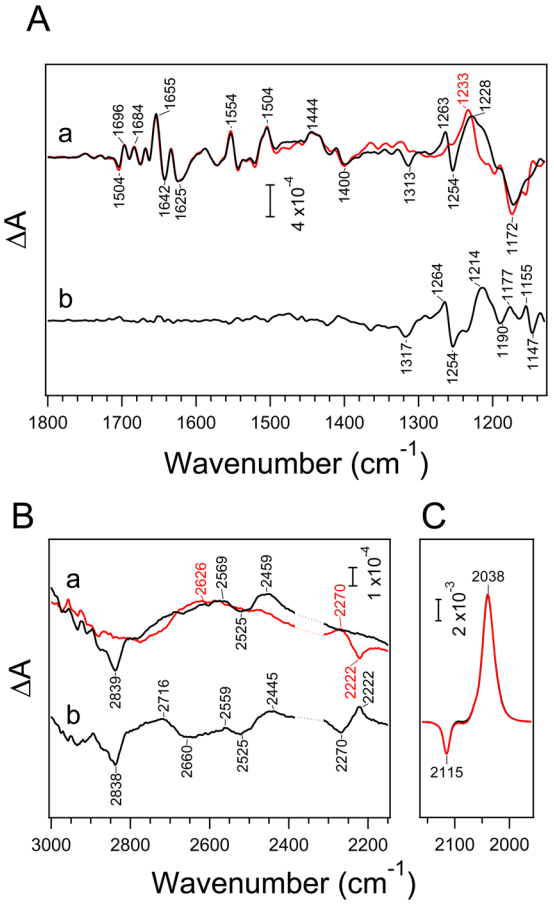

Figure 3. FTIR difference spectra of WOC upon illumination of 12 flashes on the PSII core complexes in Mes (a, black line) and Mes-d_{12} (a, red line) buffers and a Mes-minus-Mes-d_{12} double difference spectrum (b) in the regions of 1800−1130 cm^{-1} (A) and 3000−2150 cm^{-1} (B). (C) The CN stretching bands of ferricyanide (2115 cm^{-1}) and ferrocyanide (2038 cm^{-1}) in the FTIR difference spectra of WOC in Mes (black line) and Mes-d_{12} (red line). The dotted lines in panel B are the frequency region of CO_2 in atmosphere.

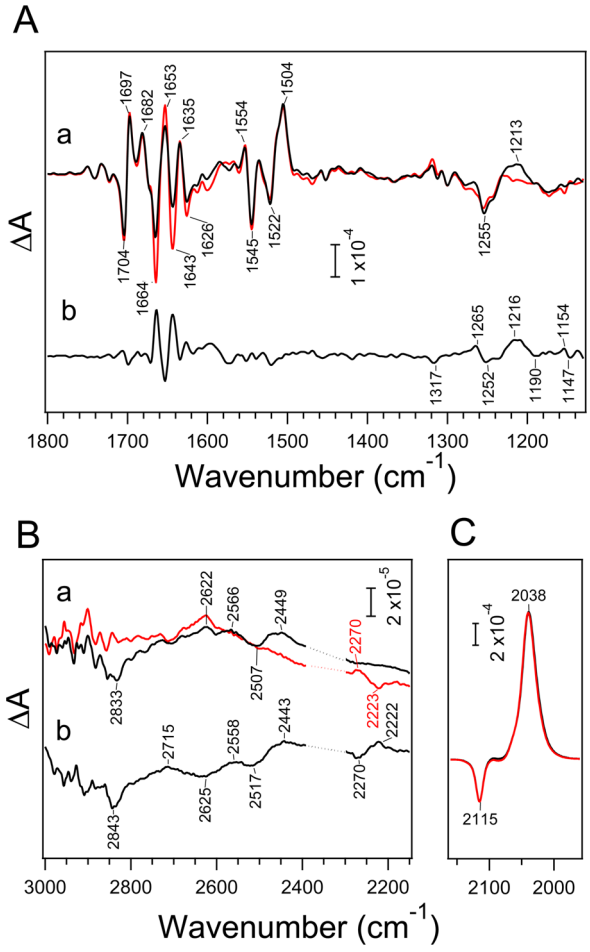

Figure 4. $Y_D^{\bullet}/Y_D$ FTIR difference spectra of the PSII core complexes in Mes (a, black line) and Mes-d_{12} (a, red line) buffers and a Mes-minus-Mes-d_{12} double difference spectrum (b) in the regions of 1800−1130 cm^{-1} (A) and 3000−2150 cm^{-1} (B). (C) The CN stretching bands of ferricyanide (2115 cm^{-1}) and ferrocyanide (2038 cm^{-1}) in the $Y_D^{\bullet}/Y_D$ difference spectra in Mes (black line) and Mes-d_{12} (red line). The dotted lines in panel B are the frequency region of CO_2 in atmosphere.

b) showed several bands in the regions of 1350−1130 and 2850−2200 cm^{-1}, very similar to those of the corresponding double difference spectrum of WOC (Figures 3A,B; trace b). Note that some bands around 1650 cm^{-1} (Figure 4A; trace b) are artifacts due to the saturation of absorption by strong amide I and water bending bands ($A \sim 1.2$) in the samples for the $Y_D^{\bullet}/Y_D$ measurement. As shown in trace b of Figure 3A, no Mes signal originated in this region.

To estimate the number of protons released from Y_D, the intensity of the Mes-minus-Mes-d_{12} double difference spectrum of WOC (Figures 3A,B; trace b) was normalized to that of Y_D (Figures 4A,B; trace b) so that the intensity of the ferricyanide band at 2115 cm^{-1} in the original difference spectrum (Figure 3C) was adjusted to that of the $Y_D^{\bullet}/Y_D$ spectrum (Figure 4C). Thus, the number of protons released from WOC and that from Y_D can be compared with respect to the same number of electrons transferred to ferricyanide on the electron acceptor side. Because an average of one proton is released from WOC per one electron transferred to ferricyanide (12 flashes are sufficient to randomize the S-state cycle), the relative intensity of the Mes signal indicates the number of protons released by the oxidation of one Y_D. In Figure 5, the normalized Mes spectra of WOC (black line) and Y_D (red line) are compared in the regions of 1350−1130 (Figure 5A) and 3000−2150 cm^{-1} (Figure 5B). The intensity ratio of the Mes signals of Y_D relative to those of WOC was estimated by fitting the spectra in the regions of 1330−1150 and 2800−2400 cm^{-1}, yielding a value of 0.84 ± 0.10. This result indicates that 0.8−0.9 protons are released into the bulk upon oxidation of one Y_D.

As a control experiment, we studied proton release into the bulk upon Y_Z oxidation. Figure 6 shows the $Y_Z^{\bullet}/Y_Z$ FTIR difference spectra in high-concentration Mes and Mes-d_{12} buffers in the regions of 1800−1130 (Figure 6A) and 3000−2150 cm^{-1} (Figure 6B) with ferricyanide/ferrocyanide peaks at 2115/2038 cm^{-1} (Figure 6C). The spectra were characterized by a positive peak at 1515 cm^{-1} arising from the CO stretching vibration of $Y_Z^{\bullet}$,[27] which was detected at a higher frequency by 11 cm^{-1} compared with the corresponding peak of $Y_D^{\bullet}$ at 1504 cm^{-1} (Figure 4A). It was shown that the spectra in Mes and Mes-d_{12} are virtually identical, which was confirmed by their double difference spectrum showing no specific bands throughout the regions (trace b in Figure 6A,B). In Figure 7, the double difference spectrum is compared with the corresponding spectrum of WOC, which was normalized with the intensity of the ferricyanide band at 2115 cm^{-1} in a way that

DOI: 10.1021/acs.biochem.5b00568
Biochemistry 2015, 54, 5045−5053

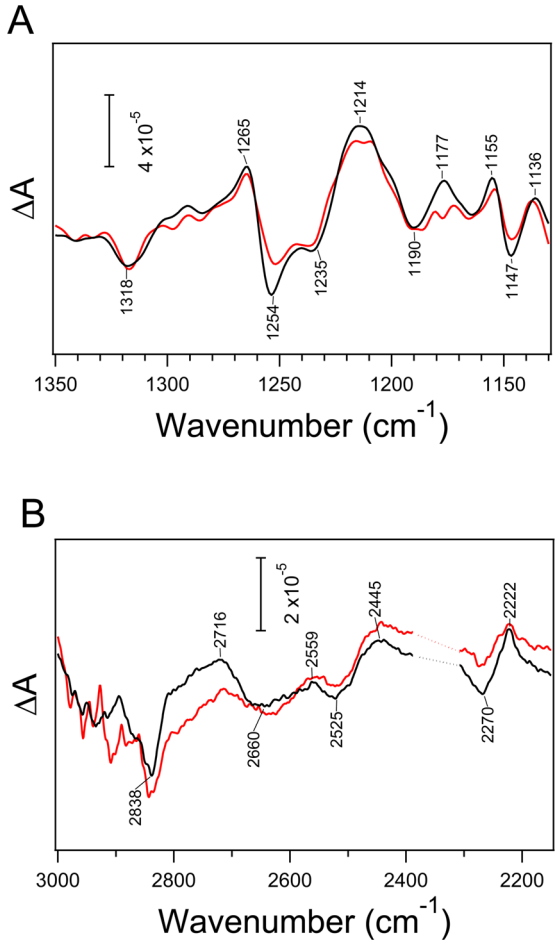

Figure 5. Comparison of the Mes-minus-Mes-d_{12} double difference spectra of WOC (black line) and $Y_D^{\bullet}/Y_D$ (red line) in the regions of 1350−1130 cm^{-1} (A) and 3000−2150 cm^{-1} (B). The intensity of the spectrum of WOC was scaled based on the intensity of the ferricyanide peak at 2115 cm^{-1} in the original difference spectrum (Figure 3C, black line) relative to that of $Y_D^{\bullet}/Y_D$ (Figure 4C, black line). The dotted lines in panel B are the frequency region of CO_2 in atmosphere.

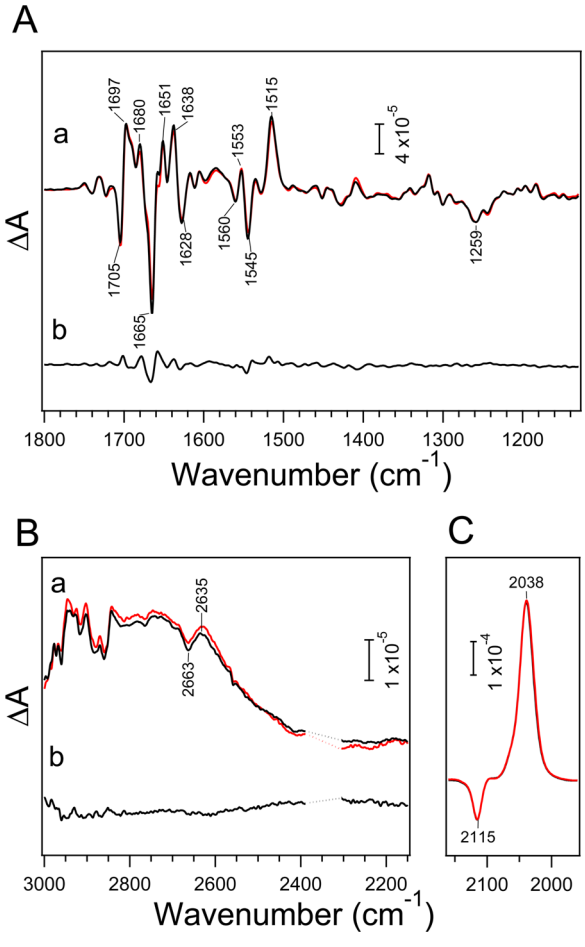

Figure 6. $Y_Z^{\bullet}/Y_Z$ FTIR difference spectra of the PSII core complexes in Mes (a, black line) and Mes-d_{12} (a, red line) buffers and a Mes-minus-Mes-d_{12} double difference spectrum (b) in the regions of 1800−1130 cm^{-1} (A) and 3000−2150 cm^{-1} (B). (C) The CN stretching bands of ferricyanide (2115 cm^{-1}) and ferrocyanide (2038 cm^{-1}) in the $Y_Z^{\bullet}/Y_Z$ difference spectra in Mes (black line) and Mes-d_{12} (red line). The dotted lines in panel B are the frequency region of CO_2 in atmosphere.

was analogous to the Y_D case. It was shown that the isotope-edited Mes bands by Y_Z oxidation are almost undetectable and, hence, significantly smaller than those of WOC. This observation confirms that a proton is virtually unreleased into the bulk when Y_Z is oxidized.

DISCUSSION

We estimated the number of protons that are released from the proteins upon oxidation of Y_D using the proton detection method that utilizes isotope-edited FTIR signals of Mes buffer (Mes-minus-Mes-d_{12}).[48] By comparing these Mes signals by Y_D oxidation with the standard Mes signals by water oxidation, we showed that 0.84 ± 0.10 protons are released into the bulk upon oxidation of Y_D (Figure 5). This result indicates that the proton of Y_D is mostly released from the proteins and is not trapped by the neighboring D2-His189 with a putative hydrogen bond with Y_D. This is consistent with our recent FTIR result showing that no N_τ−H stretching band of protonated $HisH^+$ corresponding to a broad band at ∼2800 cm^{-1} due to protonated D1-His190 in a $Y_Z^{\bullet}/Y_Z$ spectrum was detected in a $Y_D^{\bullet}/Y_D$ spectrum.[27] The absence of proton release into the bulk upon Y_Z, in contrast to Y_D, oxidation was confirmed by FTIR measurements of $Y_Z^{\bullet}/Y_Z$ in Mes and Mes-d_{12} buffers (Figure 6). The Mes-minus-Mes-d_{12} double difference spectrum showed almost no feature (Figure 7). This observation also demonstrates the validity of the proton detection method using the Mes signals.

The absence of a proton trap by the Mes buffer upon Y_Z oxidation (Figure 7) further suggests that the detection of proton release upon Y_D oxidation is not an artifact induced by high-concentration Mes buffer. In addition, previous $Y_D^{\bullet}/Y_D$ FTIR spectra measured in a lower concentration buffer at pH 6.0[37,57] showed a broad positive feature around 1720 cm^{-1}, indicative of the protonation of nonspecific carboxylate groups on the protein surface by protons released into the bulk. These observations suggest that high-concentration Mes buffer does not influence the proton release reaction from Y_D, and the number of protons detected by the Mes buffer reflects the real number of protons released from Y_D upon its oxidation. Another concern may be that Mn depletion could change the hydrogen bond network around Y_D and affect its proton release reaction. However, the $Y_D^{\bullet}/Y_D$ spectrum measured using O_2-evolving PSII (Figure S1 in Supporting Information), which was recorded after relaxation of the S_2 state by Y_D oxidation, was very similar to the spectrum of Mn-depleted PSII.

DOI: 10.1021/acs.biochem.5b00568
Biochemistry 2015, 54, 5045−5053

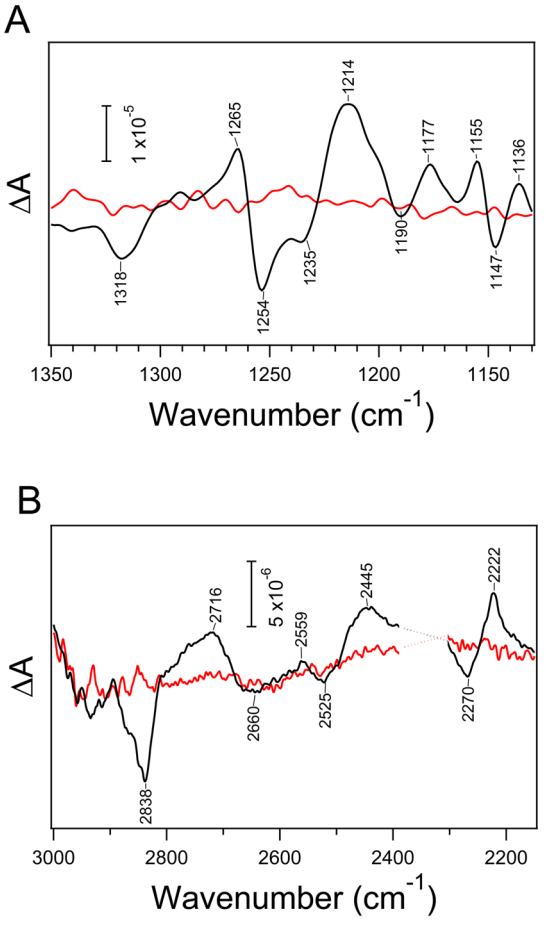

Figure 7. Comparison of the Mes-minus-Mes-d_{12} double difference spectra of WOC (black line) and $Y_Z^{\bullet}/Y_Z$ (red line) in the regions of 1350−1130 cm^{-1} (A) and 3000−2150 cm^{-1} (B). The intensity of the spectrum of WOC was scaled based on the intensity of the ferricyanide peak at 2115 cm^{-1} in the original difference spectrum (Figure 3C, black line) relative to that of $Y_Z^{\bullet}/Y_Z$ (Figure 6C, black line). The dotted lines in panel B are the frequency region of CO_2 in atmosphere.

Specifically, the CO stretching band of $Y_D^{\bullet}$ at 1504 cm^{-1} was identical between the intact and Mn-depleted PSII samples, indicating that the hydrogen bond interaction of $Y_D^{\bullet}$ is virtually unaffected by Mn deletion.

The remaining 0.1−0.2 protons, which were not detected by the Mes buffer in the bulk, may be trapped in the proteins. A previous EPR study conducted by Faller et al.[12] showed the rapid formation of $Y_D^{\bullet}$ at higher pHs with a pK_a of 7.7. Hienerwadel et al.[37] also showed in their FTIR study the change in the hydrogen bond interaction of the reduced form of Y_D with pK_a of ∼7. The presence of a proton acceptor with a pK_a of 7.0−7.7, which was speculated to be the imidazolate form of D2-His189 (see below),[17] explains the remaining proton of ∼15% at pH 6.5, the pH used in the present study.

It has been generally thought that the proton of Y_D is transferred to D2-His189, which is most probably hydrogen-bonded with Y_D,[18,26,28−31,62−64] similar to the case of Y_Z, whose proton is transferred to the neighboring D1-His190 upon its oxidation.[9,24,25,27,32−35] However, theoretical calculation by Saito et al.[17] based on the 1.9 Å resolution structure of PSII[30] showed that the proton of Y_D is not trapped by D2-His189 but moves to the hydrogen-bonded water molecule and is then transferred away from Y_D through a hydrogen bond network involving a water chain (Figure 1A). They suggested that the proton is released into the bulk via D2-His61 located in the proton pathway. Our FTIR data showing proton detection in the bulk upon Y_D oxidation is in agreement with this theoretical prediction and hence supports the proton release process proposed by Saito et al.[17]

The clear difference in the proton transfer reactions between Y_Z and Y_D arises from the difference in the hydrogen-bonded structures of these Tyr side chains, the coupled His (D1-His190 and D2-His189, respectively), and the amino acid residue hydrogen-bonded to the N_π site of this His (Figure 8). Whereas

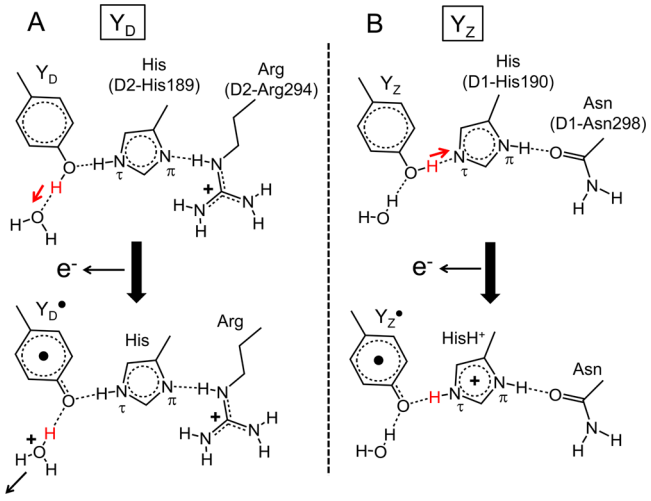

Figure 8. Schematic picture of the hydrogen-bonded structures of Y_D-His (A) and Y_Z-His (B) and the proton transfer reactions upon oxidation.

the amide C═O of D1-Asn298 interacts with D1-His190 as a hydrogen bond acceptor (Figure 8B), D2-Arg294, which most probably has a guanidinium cation form, donates a hydrogen bond to D2-His189 coupled to Y_D. Because of these different hydrogen bond interactions of D1-Asn298 and D2-Arg294 at the N_π site, D1-His190 and D2-His189, in turn, function as a hydrogen bond acceptor and donor, respectively, to the phenolic oxygen of Tyr.[17,27] Thus, whereas the proton of Y_Z is transferred to D1-His190 through a hydrogen bond, the proton of Y_D cannot be transferred to D1-His189, which is already protonated at the N_τ site, but it is transferred to a hydrogen-bonded water molecule, leading to a long-distance proton transfer (Figure 8).[17] The presence of such a water molecule interacting with Y_D was also detected by the previous FTIR measurement.[54] The hydrogen bond network from Y_D to the luminal side via D2-Arg180 and D2-His61 (Figure 1A), involving the movement of a hydronium cation from Y_D to D2-Arg180 shown in the quantum mechanics/molecular mechanics (QM/MM) study of Saito et al.,[17] may be used for the proton release pathway upon Y_D oxidation. Site-directed mutants at D2-Arg180 showed significant alterations of the EPR signal of $Y_D^{\bullet}$, indicating a strong interaction between Y_D and D2-Arg180,[36] and it was recently shown that a water molecule between Y_D and D2-Arg180 is important for the H/D exchange of Y_D.[65] These observations also support the significance of the hydrogen bond network via D2-Arg180 as a proton pathway from Y_D to the bulk.[17]

Oxidation and rereduction of Y_D slower than that of Y_Z[10−13] can be explained by this long-distance proton transfer for Y_D,

DOI: 10.1021/acs.biochem.5b00568
Biochemistry 2015, 54, 5045−5053

providing a high-energy barrier in the reaction coordinate,[17] in contrast to the short proton transfer for Y_Z through a strong hydrogen bond, which requires almost no energy barrier.[24] Previous observations of the fast redox reaction and low-temperature oxidation of Y_D at high pH values[12,19,20,22] are explained by deprotonation of D2-His189 to be an imidozolate anion form inducing rapid proton transfer from Y_D to D2-His189 without proton release into the bulk.[17] In addition, the lower E_m value of Y_D (+700−800 mV)[11,66] than that of Y_Z (+900−1000 mV)[11,67] may be partly attributed to the stabilization of the oxidized form of Y_D due to an entropy increase by the diffusion of a proton into the bulk, in addition to the electrostatic effects of partial charges in the protein moieties.[68]

In conclusion, we provided experimental evidence that the proton of Y_D is released from the protein upon its oxidation, supporting the previous QM/MM study by Saito et al.[17] This long-distance proton transfer should significantly contribute to the functional difference between Y_D and Y_Z. The key amino acid residues controlling the hydrogen-bonded structures and proton transfer reactions of Y_D and Y_Z are D2-Arg294 and D1-Asn298 interacting with the coupled His as a hydrogen bond donor and acceptor, respectively, in the Y_D-His-Arg and Y_Z-His-Asn triads.

■ ASSOCIATED CONTENT

Supporting Information

The Supporting Information is available free of charge on the ACS Publications website at DOI: 10.1021/acs.biochem.5b00568.

$Y_D^{\bullet}/Y_D$ FTIR difference spectra of O_2-evolving PSII complexes (PDF)

■ AUTHOR INFORMATION

Corresponding Author

*E-mail: tnoguchi@bio.phys.nagoya-u.ac.jp. Telephone: +81-52-789-2881. Fax: +81-52-789-2883.

Funding

This study was supported by the Grants-in-Aids for JSPS Fellows (15J10320 to S.N.) and for Scientific Research from the Ministry of Education, Culture, Sports, Science and Technology (24000018, 24107003, and 25291033 to T.N.).

Notes

The authors declare no competing financial interest.

■ ABBREVIATIONS

DM, *n*-dodecyl *β*-D-maltoside; FTIR, Fourier transform infrared; Mes, 2-(*N*-morpholino)ethanesulfonic acid; PSII, photosystem II; P680, special pair chlorophyll of photosystem II; WOC, water-oxidizing center; Y_D, redox-active tyrosine on the D2 subunit (D2-Tyr160) of photosystem II; Y_Z, redox-active tyrosine on the D1 subunit (D1-Tyr161) of photosystem II

■ REFERENCES

(1) Diner, B. A., and Rappaport, F. (2002) Structure, dynamics, and energetics of the primary photochemistry of photosystem II of oxygenic photosynthesis. *Annu. Rev. Plant Biol. 53*, 551−580.

(2) Renger, G., and Holzwarth, A. R. (2005) Primary electron transfer. In *Photosystem II: The Light-Driven Water:Plastoquinone Oxidoreductase* (Wydrzynski, T. and Satoh, K., Eds.) pp 139−175, Springer, Dordrecht, The Netherlands.

(3) Diner, B., and Britt, R. D. (2005) The redox-active tyrosine Y_Z and Y_D. In *Photosystem II: The Light-Driven Water:Plastoquinone Oxidoreductase* (Wydrzynski, T. and Satoh, K., Eds.) pp 207−233, Springer, Dordrecht, The Netherlands.

(4) Renger, G., and Renger, T. (2008) Photosystem II: The machinery of photosynthetic water splitting. *Photosynth. Res. 98*, 53−80.

(5) Rappaport, F., Blanchard-Desce, M., and Lavergne, J. (1994) Kinetics of electron transfer and electrochromic change during the redox transitions of the photosynthetic oxygen-evolving complex. *Biochim. Biophys. Acta, Bioenerg. 1184*, 178−192.

(6) Haumann, M., Liebisch, P., Müller, C., Barra, M., Grabolle, M., and Dau, H. (2005) Photosynthetic O_2 formation tracked by time-resolved X-ray experiments. *Science 310*, 1019−1021.

(7) Noguchi, T., Suzuki, H., Tsuno, M., Sugiura, M., and Kato, C. (2012) Time-resolved infrared detection of the proton and protein dynamics during photosynthetic oxygen evolution. *Biochemistry 51*, 3205−3214.

(8) Klauss, A., Haumann, M., and Dau, H. (2015) Seven steps of alternating electron and proton transfer in photosystem II water oxidation traced by time-resolved photothermal beam deflection at improved sensitivity. *J. Phys. Chem. B 119*, 2677−2689.

(9) Styring, S., Sjöholm, J., and Mamedov, F. (2012) Two tyrosines that changed the world: Interfacing the oxidizing power of photochemistry to water splitting in photosystem II. *Biochim. Biophys. Acta, Bioenerg. 1817*, 76−87.

(10) Styring, S., and Rutherford, A. W. (1987) In the oxygen-evolving complex of Photosystem II the S_0 state is oxidized to the S_1 state by D^+ (Signal II slow). *Biochemistry 26*, 2401−2405.

(11) Vass, I., and Styring, S. (1991) pH-Dependent charge equilibria between tyrosine-D and the S states in photosystem II. Estimation of relative midpoint redox potentials. *Biochemistry 30*, 830−839.

(12) Faller, P., Debus, R. J., Brettel, K., Sugiura, M., Rutherford, A. W., and Boussac, A. (2001) Rapid formation of the stable tyrosyl radical in photosystem II. *Proc. Natl. Acad. Sci. U. S. A. 98*, 14368−14373.

(13) Buser, C. A., Thompson, L. K., Diner, B. A., and Brudvig, G. W. (1990) Electron-transfer reactions in manganese-depleted photosystem II. *Biochemistry 29*, 8977−8985.

(14) Magnuson, A., Rova, M., Mamedov, F., Fredriksson, P. O., and Styring, S. (1999) The role of cytochrome b_{559} and tyrosine$_D$ in protection against photoinhibition during in vivo photoactivation of photosystem II. *Biochim. Biophys. Acta, Bioenerg. 1411*, 180−191.

(15) Ananyev, G. M., Sakiyan, I., Diner, B. A., and Dismukes, G. C. (2002) A functional role for tyrosine-D in assembly of the inorganic core of the water oxidase complex of photosystem II and the kinetics of water oxidation. *Biochemistry 41*, 974−980.

(16) Rutherford, A. W., Boussac, A., and Faller, P. (2004) The stable tyrosyl radical in photosystem II: why D? *Biochim. Biophys. Acta, Bioenerg. 1655*, 222−230.

(17) Saito, K., Rutherford, A. W., and Ishikita, H. (2013) Mechanism of tyrosine D oxidation in Photosystem II. *Proc. Natl. Acad. Sci. U. S. A. 110*, 7690−7695.

(18) Babcock, G. T., Barry, B. A., Debus, R. J., Hoganson, C. W., Atamian, M., McIntosh, L., Sithole, I., and Yocum, C. F. (1989) Water oxidation in photosystem II: From radical chemistry to multielectron chemistry. *Biochemistry 28*, 9557−9565.

(19) Faller, P., Rutherford, A. W., and Debus, R. J. (2002) Tyrosine D oxidation at cryogenic temperature in photosystem II. *Biochemistry 41*, 12914−12920.

(20) Faller, P., Goussias, C., Rutherford, A. W., and Un, S. (2003) Resolving intermediates in biological proton-coupled electron transfer: a tyrosyl radical prior to proton movement. *Proc. Natl. Acad. Sci. U. S. A. 100*, 8732−8735.

(21) Berthomieu, C., and Hienerwadel, R. (2005) Vibrational spectroscopy to study the properties of redox-active tyrosines in photosystem II and other proteins. *Biochim. Biophys. Acta, Bioenerg. 1707*, 51−66.

DOI: 10.1021/acs.biochem.5b00568
Biochemistry 2015, 54, 5045−5053

(22) Havelius, K. G. V., and Styring, S. (2007) pH dependent competition between Y_Z and Y_D in photosystem II probed by illumination at 5 K. *Biochemistry 46*, 7865−7874.
(23) Hammarström, L., and Styring, S. (2011) Proton-coupled electron transfer of tyrosines in Photosystem II and model systems for artificial photosynthesis: the role of a redox-active link between catalyst and photosensitizer. *Energy Environ. Sci. 4*, 2379−2388.
(24) Saito, K., Shen, J.-R., Ishida, T., and Ishikita, H. (2011) Short hydrogen bond between redox-active tyrosine Y_Z and D1-His190 in the photosystem II crystal structure. *Biochemistry 50*, 9836−9844.
(25) Matsuoka, H., Shen, J.-R., Kawamori, A., Nishiyama, K., Ohba, Y., and Yamauchi, S. (2011) Proton-coupled electron-transfer processes in photosystem II probed by highly resolved *g*-anisotropy of redox-active tyrosine Y_Z. *J. Am. Chem. Soc. 133*, 4655−4660.
(26) Chatterjee, R., Coates, C. S., Milikisiyants, S., Lee, C.-I., Wagner, A., Poluektov, O. G., and Lakshmi, K. V. (2013) High-frequency electron nuclear double-resonance spectroscopy studies of the mechanism of proton-coupled electron transfer at the tyrosine-D residue of photosystem II. *Biochemistry 52*, 4781−4790.
(27) Nakamura, S., Nagao, R., Takahashi, R., and Noguchi, T. (2014) Fourier transform infrared detection of a polarizable proton trapped between photooxidized tyrosine Y_Z and a coupled histidine in photosystem II: relevance to the proton transfer mechanism of water oxidation. *Biochemistry 53*, 3131−3144.
(28) Ferreira, K. N., Iverson, T. M., Maghlaoui, K., Barber, J., and Iwata, S. (2004) Architecture of the photosynthetic oxygen-evolving center. *Science 303*, 1831−1838.
(29) Guskov, A., Kern, J., Gabdulkhakov, A., Broser, M., Zouni, A., and Saenger, W. (2009) Cyanobacterial photosystem II at 2.9-Å resolution and the role of quinones, lipids, channels and chloride. *Nat. Struct. Mol. Biol. 16*, 334−342.
(30) Umena, Y., Kawakami, K., Shen, J.-R., and Kamiya, N. (2011) Crystal structure of oxygen-evolving photosystem II at a resolution of 1.9 Å. *Nature 473*, 55−60.
(31) Suga, M., Akita, F., Hirata, K., Ueno, G., Murakami, H., Nakajima, Y., Shimizu, T., Yamashita, K., Yamamoto, M., Ago, H., and Shen, J.-R. (2015) Native structure of photosystem II at 1.95 Å resolution viewed by femtosecond X-ray pulses. *Nature 517*, 99−103.
(32) Rappaport, F., and Lavergne, J. (2001) Coupling of electron and proton transfer in the photosynthetic water oxidase. *Biochim. Biophys. Acta, Bioenerg. 1503*, 246−259.
(33) Rappaport, F., Boussac, A., Force, D. A., Peloquin, J., Brynda, M., Sugiura, M., Un, S., Britt, R. D., and Diner, B. A. (2009) Probing the coupling between proton and electron transfer in photosystem II core complexes containing a 3-fluorotyrosine. *J. Am. Chem. Soc. 131*, 4425−4433.
(34) Ahlbrink, R., Haumann, M., Cherepanov, D., Bögershausen, O., Mulkidjanian, A., and Junge, W. (1998) Function of tyrosine Z in water oxidation by photosystem II: Electrostatical promotor instead of hydrogen abstractor. *Biochemistry 37*, 1131−1142.
(35) Hays, A. M. A., Vassiliev, I. R., Golbeck, J. H., and Debus, R. J. (1999) Role of D1-His190 in the proton-coupled oxidation of tyrosine Y_Z in manganese-depleted photosystem II. *Biochemistry 38*, 11851−11865.
(36) Manna, P., LoBrutto, R., Eijckelhoff, C., Dekker, J. P., and Vermaas, W. (1998) Role of Arg180 of the D2 protein in photosystem II structure and function. *Eur. J. Biochem. 251*, 142−154.
(37) Hienerwadel, R., Diner, B. A., and Berthomieu, C. (2008) Molecular origin of the pH dependence of tyrosine D oxidation kinetics and radical stability in photosystem II. *Biochim. Biophys. Acta, Bioenerg. 1777*, 525−531.
(38) Chu, H.-A., Hillier, W., Law, N. A., and Babcock, G. T. (2001) Vibrational spectroscopy of the oxygen-evolving complex and of manganese model compounds. *Biochim. Biophys. Acta, Bioenerg. 1503*, 69−82.
(39) Noguchi, T., and Berthomieu, C. (2005) Molecular analysis by vibrational spectroscopy. In *Photosystem II: The Light-Driven Water:-Plastoquinone Oxidoreductase* (Wydrzynski, T. and Satoh, K., Eds.) pp 367−387, Springer, Dordrecht, The Netherlands.
(40) Noguchi, T. (2007) Light-induced FTIR difference spectroscopy as a powerful tool toward understanding the molecular mechanism of photosynthetic oxygen evolution. *Photosynth. Res. 91*, 59−69.
(41) Debus, R. J. (2008) Protein ligation of the photosynthetic oxygen-evolving center. *Coord. Chem. Rev. 252*, 244−258.
(42) Noguchi, T. (2008) Fourier transform infrared analysis of the photosynthetic oxygen-evolving center. *Coord. Chem. Rev. 252*, 336−346.
(43) Berthomieu, C., and Hienerwadel, R. (2009) Fourier transform infrared (FTIR) spectroscopy. *Photosynth. Res. 101*, 157−170.
(44) Noguchi, T. (2013) Monitoring the reactions of photosynthetic water oxidation using infrared spectroscopy. *Biomed. Spectrosc. Imaging 2*, 115−128.
(45) Chu, H.-A. (2013) Fourier transform infrared difference spectroscopy for studying the molecular mechanism of photosynthetic water oxidation. *Front. Plant Sci. 4*, 146.
(46) Debus, R. J. (2015) FTIR studies of metal ligands, networks of hydrogen bonds, and water molecules near the active site Mn_4CaO_5 cluster in Photosystem II. *Biochim. Biophys. Acta, Bioenerg. 1847*, 19−34.
(47) Noguchi, T. (2015) Fourier transform infrared difference and time-resolved infrared detection of the electron and proton transfer dynamics in photosynthetic water oxidation. *Biochim. Biophys. Acta, Bioenerg. 1847*, 35−45.
(48) Suzuki, H., Sugiura, M., and Noguchi, T. (2009) Monitoring proton release during photosynthetic water oxidation in photosystem II by means of isotope-edited infrared spectroscopy. *J. Am. Chem. Soc. 131*, 7849−7857.
(49) Iwai, M., Suzuki, T., Kamiyama, A., Sakurai, I., Dohmae, N., Inoue, Y., and Ikeuchi, M. (2010) The PsbK subunit is required for the stable assembly and stability of other small subunits in the PSII complex in the thermophilic cyanobacterium *Thermosynechococcus elongatus* BP-1. *Plant Cell Physiol. 51*, 554−560.
(50) Noguchi, T., and Sugiura, M. (2002) Flash-induced FTIR difference spectra of the water oxidizing complex in moderately hydrated photosystem II core films: Effect of hydration extent on S-state transitions. *Biochemistry 41*, 2322−2330.
(51) Hienerwadel, R., and Berthomieu, C. (1995) Bicarbonate binding to the non-heme iron of photosystem II investigated by FTIR difference spectroscopy and ^{13}C-labeled bicarbonate. *Biochemistry 34*, 16288−16297.
(52) Noguchi, T., and Inoue, Y. (1995) Identification of FTIR signals from the non-heme iron in photosystem II. *J. Biochem. 118*, 9−12.
(53) Berthomieu, C., and Hienerwadel, R. (2001) Iron coordination in photosystem II: interaction between bicarbonate and the Q_B pocket studied by Fourier transform infrared spectroscopy. *Biochemistry 40*, 4044−4052.
(54) Takahashi, R., Sugiura, M., and Noguchi, T. (2007) Water molecules coupled to the redox-active tyrosine Y_D in photosystem II as detected by FTIR spectroscopy. *Biochemistry 46*, 14245−14249.
(55) Noguchi, T., and Sugiura, M. (2002) FTIR detection of water reactions during the flash-induced S-state cycle of the photosynthetic water oxidizing complex. *Biochemistry 41*, 15706−15712.
(56) Hienerwadel, R., Boussac, A., Breton, J., and Berthomieu, C. (1996) Fourier transform infrared difference study of tyrosine$_D$ oxidation and plastoquinone Q_A reduction in photosystem II. *Biochemistry 35*, 15447−15460.
(57) Hienerwadel, R., Boussac, A., Breton, J., Diner, B. A., and Berthomieu, C. (1997) Fourier transform infrared difference spectroscopy of photosystem II tyrosine D using site-directed mutagenesis and specific isotope labeling. *Biochemistry 36*, 14712−14723.
(58) Hienerwadel, R., Gourion-Arsiquaud, S., Ballottari, M., Bassi, R., Diner, B. A., and Berthomieu, C. (2005) Formate binding near the redox-active Tyrosine$_D$ in Photosystem II: consequences on the properties of Tyr$_D$. *Photosynth. Res. 84*, 139−144.
(59) Noguchi, T., Inoue, Y., and Tang, X.-S. (1997) Structural coupling between the oxygen-evolving Mn cluster and a tyrosine residue in photosystem II as revealed by Fourier transform infrared spectroscopy. *Biochemistry 36*, 14705−14711.

DOI: 10.1021/acs.biochem.5b00568
Biochemistry 2015, 54, 5045−5053

(60) Chu, H.-A., Hillier, W., and Debus, R. J. (2004) Evidence that the C-terminus of the D1 polypeptide of photosystem II is ligated to the manganese ion that undergoes oxidation during the S_1 to S_2 transition: An isotope-edited FTIR study. *Biochemistry 43*, 3152−3166.
(61) Takahashi, R., and Noguchi, T. (2007) Criteria for determining the hydrogen-bond structures of a tyrosine side chain by Fourier transform infrared spectroscopy: Density functional theory analyses of model hydrogen-bonded complexes of *p*-cresol. *J. Phys. Chem. B 111*, 13833−13844.
(62) Tommos, C., Davidsson, L., Svensson, B., Madsen, C., Vermaas, W., and Styring, S. (1993) Modified EPR spectra of the tyrosine$_D$ radical in photosystem II in site-directed mutants of *Synechocystis* sp. PCC 6803: Identification of side chains in the immediate vicinity of tyrosine$_D$ on the D2 protein. *Biochemistry 32*, 5436−5441.
(63) Tang, X.-S., Chisholm, D. A., Dismukes, G. C., Brudvig, G. W., and Diner, B. A. (1993) Spectroscopic evidence from site-directed mutants of *Synechocystis* PCC6803 in favor of a close interaction between histidine 189 and redox-active tyrosine 160, both of polypeptide D2 of the photosystem II reaction center. *Biochemistry 32*, 13742−13748.
(64) Kessen, S., Teutloff, C., Kern, J., Zouni, A., and Bittl, R. (2010) High-Field ^{2}H-mims-ENDOR spectroscopy on PSII single crystals: Hydrogen bonding of $Y_D^{\bullet}$. *ChemPhysChem 11*, 1275−1282.
(65) Sjöholm, J., Mamedov, F., and Styring, S. (2014) Spectroscopic evidence for a redox-controlled proton gate at tyrosine D in Photosystem II. *Biochemistry 53*, 5721−5723.
(66) Boussac, A., and Etienne, A. L. (1984) Midpoint potential of signal II (slow) in Tris-washed photosystem II particles. *Biochim. Biophys. Acta, Bioenerg. 766*, 576−581.
(67) Metz, J. G., Nixon, P. J., Rögner, M., Brudvig, G. W., and Diner, B. A. (1989) Directed alteration of the D1 polypeptide of photosystem II: Evidence that tyrosine-161 is the redox component, Z, connecting the oxygen-evolving complex to the primary electron-donor, P680. *Biochemistry 28*, 6960−6969.
(68) Ishikita, H., and Knapp, E. W. (2006) Function of redox-active tyrosine in photosystem II. *Biophys. J. 90*, 3886−3896.

DOI: 10.1021/acs.biochem.5b00568
Biochemistry 2015, 54, 5045−5053